Supplement of Ocean Sci., 15, 925–940, 2019
https://doi.org/10.5194/os-15-925-2019-supplement

Ocean Science Open Access EGU

Supplement of

Segmented flow coil equilibrator coupled to a proton-transfer-reaction mass spectrometer for measurements of a broad range of volatile organic compounds in seawater

Charel Wohl et al.

Correspondence to: Mingxi Yang (miya@pml.ac.uk)

Supplementary material S1: PTR-MS Settings

To measure the VOC concentrations, we use a commercially available high sensitivity Proton-Transfer-Reaction Mass Spectrometer (de Gouw and Warneke, 2007; Lindinger and Jordan, 1998). Briefly, water vapor is ionised in a Hollow cathode DC plasma discharge. The hydronium ions react with sample air in the drift tube. Here, gases with a proton affinity higher than water, including many VOCs, are ionised continuously usually without fragmentation. Hydronium ions are in large excess of the VOCs, which allows for application of pseudo-first order kinetics in the drift tube. Together with relatively well-studied reaction rates between VOCs and hydronium ions (Zhao and Zhang, 2004) and mass spectrometer specific parameters (Yang et al., 2013), the mixing ratios of the VOCs can be fairly accurately computed without the need of an internal standard (Lindinger and Jordan, 1998). Nevertheless, reaction rate constants between VOCs and hydronium ions have a reported error margin of up to 50% (Blake et al., 2009; Ellis and Mayhew, 2014). To account for this, dynamic gas phase calibrations were carried out using a certified gas standard (see Section 2.2).

The PTR-MS is deployed in selective ion mode. Ions monitored at m/z 33, 45, 59, 63, 69, 79 and 93 were attributed to methanol, acetaldehyde, acetone, dimethyl sulphide, isoprene, benzene and toluene in accordance with previous mass assignments (Williams et al., 2001; Warneke et al., 2003). Propanal has previously been shown to have a very minor contribution to m/z 59 (Beale et al., 2013). For methanol, we correct for the oxygen isotope ($O^{18}O^{2+}$) interference by monitoring O_2^+ in the drift tube and applying a theoretical isotopic distribution ratio, which is 0.076% of the O_2^+ signal.

When measuring dissolved VOCs with the SFCE, the equilibrator headspace is laden with humidity. Previous observations suggest that humidity in the sample affects the PTR-MS drift tube kinetics through the formation of hydronium water clusters. In practice, water dimmers are monitored at m/z 37 (i.e. isotopic hydronium water cluster ($H_2{}^{18}O^+$)H_2O) as a percentage of the primary ion count, accounting for isotopic abundance of oxygen as above (Blake et al., 2009):

$$\mathrm{H_2O} + \mathrm{H_3O^+} \rightarrow \mathrm{H_3O^+(H_2O)}\,. \qquad (S1)$$

Humidity has several potential effects on the measurement: (i) The additional water molecule stabilises the primary ion by sharing the positive charge thus increasing its proton affinity (Blake et al., 2009). For example in this setup, benzene and toluene possess intermediate proton affinities and are ionised by the primary ion, but not the water cluster (Warneke et al., 2001). On the other hand, this process decreases the proton affinity difference between the primary ion and the VOCs and so the excess energy released on proton transfer reaction (de Gouw and Warneke, 2007). This leads to less fragmentation for example of isoprene in the drift tube (Schwarz et al. 2009). (ii) sample humidity affects the backgrounds of some of the VOCs monitored (de Gouw and Warneke, 2007) (Supplementary material B). (iii) Some PTR-MS have a collision-induced dissociation (CID) chamber at the end of the drift tube in which the E/N is briefly raised to simplify the mass spectra and remove humidity induced clusters which leads to an overestimation of the true hydronium primary ion concentration in the drift tube and thus an overestimation of VOC concentrations (Blake et al., 2009). However, our PTR-MS instrument does not have a CID chamber.

Clearly, excessive water clustering in the drift tube is undesirable. To keep the water dimer to be < 5% of the primary ion count when measuring the SFCE headspace, the PTR-MS drift tube was operated at 160Td (700V, 2.2 mBar and 80°C in the drift tube). The water vapor flow into the source was set to 5 cm^3n/min, the source current at 3 mA and the source valve to 35%. At these settings, the amount of hydronium water clusters is below 1% when measuring dry zero air and the amount of O_2^+ ions is below 0.7% of the primary ion counts. Residual water clusters measured during dry canister measurement is due to unionised water vapor from the hollow cathode entering the drift tube (Warneke et al., 2001). The disadvantage of this high drift tube voltage are increased fragmentation and a reduced reaction time in the drift tube leading to overall lower sensitivity. In this case these were acceptable trade-offs since the focus of these measurements are low molecular weight OVOCs that generally do not fragment. The decrease in sensitivity is captured through regular gas phase calibrations.

We maintain a constant humidity in SFCE headspace (monitored at m/z of 37) by keeping the SFCE at 20°C, regardless of the incoming water temperature. This greatly simplifies the corrections needed for the effect of humidity on the PTR-MS signal. A Nafion dryer (e.g. Nafion) has been successfully used in the measurements of seawater DMS (Blomquist et al., 2010) and would reduce many of the aforementioned measurement uncertainties. However Nafion dryers are known to remove very soluble/reactive OVOCs (Kameyama et al., 2010) and thus are not an option for these measurements.

Supplementary material S2: Humidity experiments and fragmentation experiments

To investigate the effect of humidity on the background, zero air at different humidities was measured. VOC-free air saturated in water is generated by passing synthetic air (BTCA grade) through the SFCE wetted with MilliQ water at 20°C. The concentration of water vapor was calculated to be 22.9 millimole water vapor per mole of air. This air is scrubbed with a Pt-Catalyst to oxidize all VOCs to CO_2. The high efficiency of this catalyst at oxidizing VOCs in wet and dry air is demonstrated elsewhere (Yang and Fleming, 2019) and it was found that the catalyst did not affect the humidity level. The water drain of the SFCE was capped for this experiment to balance out the pressure resistance provided by the Pt-Catalyst. This flow of scrubbed moist air is dynamically diluted with dry zero air to generate VOC-free air at different humidities.

Measurement of zero air at different humidities showed an exponential dependence of the DMS (m/z 63) and toluene (m/z 79) backgrounds to the humidity of the sample air (Fig. S2). The backgrounds of the other compounds presented here remained unaffected by humidity. Here, a measured m/z 37 of 1% corresponds to dry canister air measurement. A m/z 37 between 1.4% and 2.0% corresponds to outside air measurements and m/z 37 of 2.2% corresponds to measurements of equilibrator headspace. The equilibrator headspace is expected to contain 19.1 millimole water vapor per mole of air as a result of the 20 cm^3 min^{-1} dilution flow.

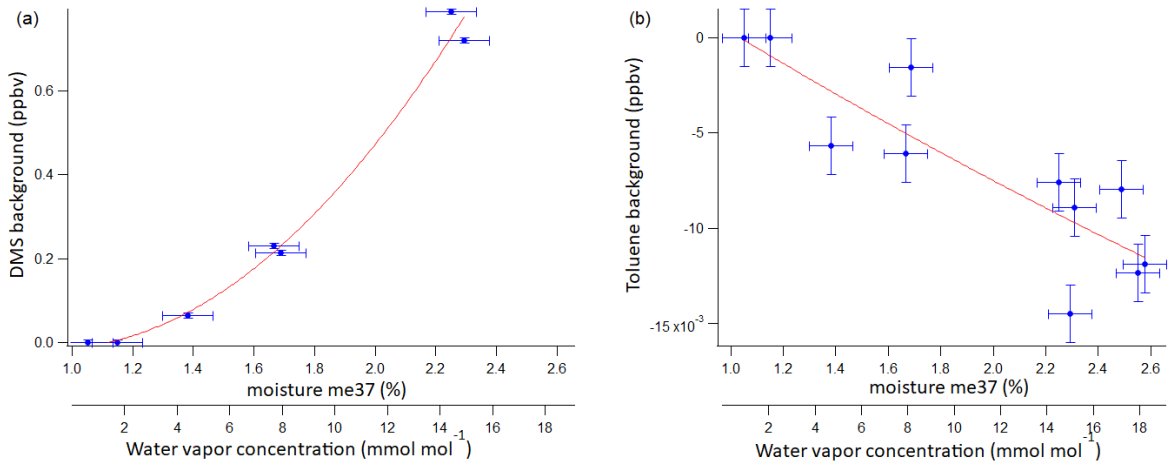

Figure S2: Background dependence of DMS (a) and toluene (b) signal on the humidity in the sample air. For this analysis, dry zero air has been subtracted already and thus the backgrounds shown here are the additional contributions due to sample humidity. Error bars represent the standard deviation of ten consecutive blanks.

Water vapor concentration and %m/z37 correlate linearly, thus both variables can be plotted on the same axis for comparison (Fig. S2). Lines of best fit for toluene and DMS background (in ppbv) as a function of the additional hydronium water cluster in the drift tube due to sample humidity (in % m/z37 of m/z21) was found to be;

$$ppb(DMS) = 0.351 - 0.789\,\{\%\mathrm{m/z}\,37\} + 0.425\,\{\%\mathrm{m/z}\,37\}^2 \qquad (S2)$$

$$ppb(toluene) = 0.00909 - 0.00932\,\{\%\mathrm{m/z}\,37\} + 0.000513\,\{\%\mathrm{m/z}\,37\}^2 \qquad (S3)$$

During this experiment, the source water flow in the PTR-MS was kept constant, and the zero air measurement has been subtracted to remove the contribution to the VOC signals from the PTR-MS source water reservoir. Variations in the measured background are thus due to the sample humidity alone. These results suggest that using zero air (e.g. bypassing the SFCE) as the background could lead to overestimations of dissolved DMS and underestimations of dissolved toluene.

In a separate experiment, the flow of water vapor into the PTR-MS source was varied while measuring dry zero air to simulate the influence of humidity induced water clusters on the background of the measurement. The backgrounds of all the masses monitored changed and significantly increased for the soluble OVOCs (methanol, acetone, acetaldehyde) with increasing source water flow. This suggests that the backgrounds in the measurements of these compounds are significantly affected by residual OVOCs in the water reservoir.

Furthermore, dynamic gas phase calibrations at different humidity levels were carried out. For this, mass flow controllers were used to dilute a flow of zero air at different moistures (BTCA air scrubbed by Pt-catalyst) and a gravimetrically prepared standard gas in ultrapure N_2 with known amount of VOC (517 ppbv acetaldehyde, 490 ppbv methanol, 512 ppbv acetone, 491 ppbv isoprene, 527 ppbv DMS, 500 ppbv benzene, 483 ppbv toluene, Apel–Riemer Environmental Inc., Miami, Florida, USA). The ratio between synthetic air and VOC standard in N_2 was typically more than 10:1, thus not significantly changing the matrix.

For most of the VOCs, the calibration slopes did not vary with humidity at the settings chosen. However, benzene, toluene and isoprene did show some humidity dependence (Fig. S3–Fig. S5).

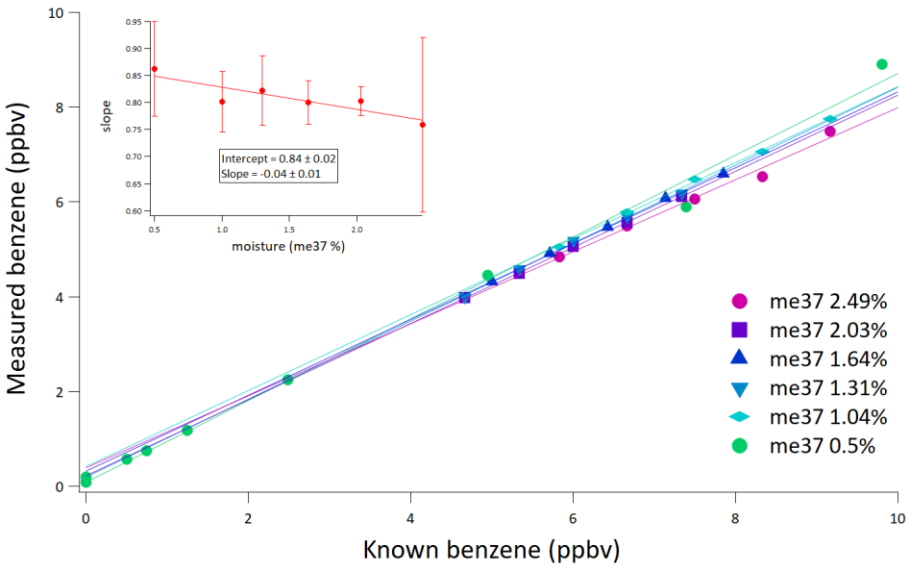

Figure S3: Benzene gas phase calibrations at different humidities and the dependency of the slope on the measured humidity as an inset. Error bars on the slope and intercept represent 95% confidence intervals of the linear regression.

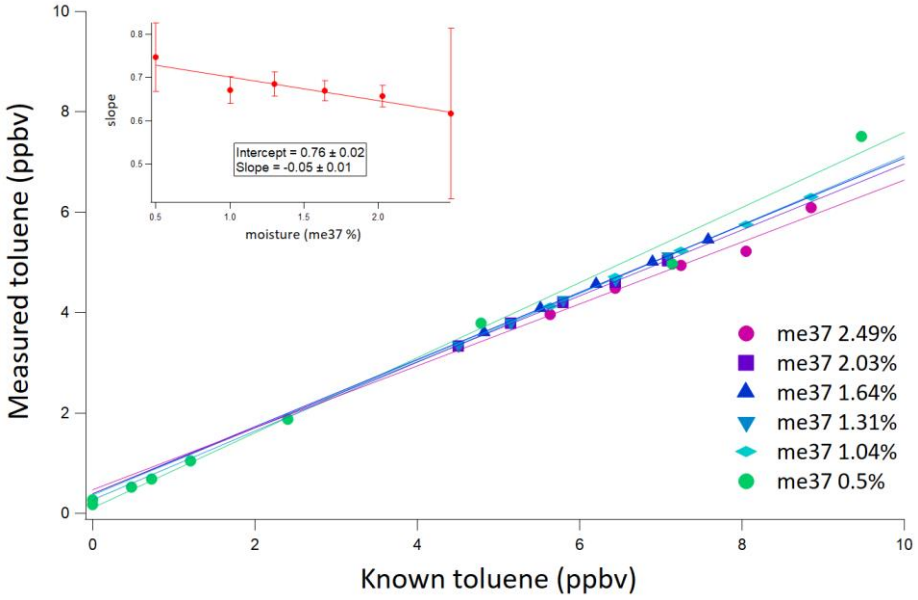

Figure S4: Toluene gas phase calibrations at different humidities and the dependency of the slope on the measured humidity as an inset. Error bars on the slope and intercept represent 95% confidence intervals of the linear regression.

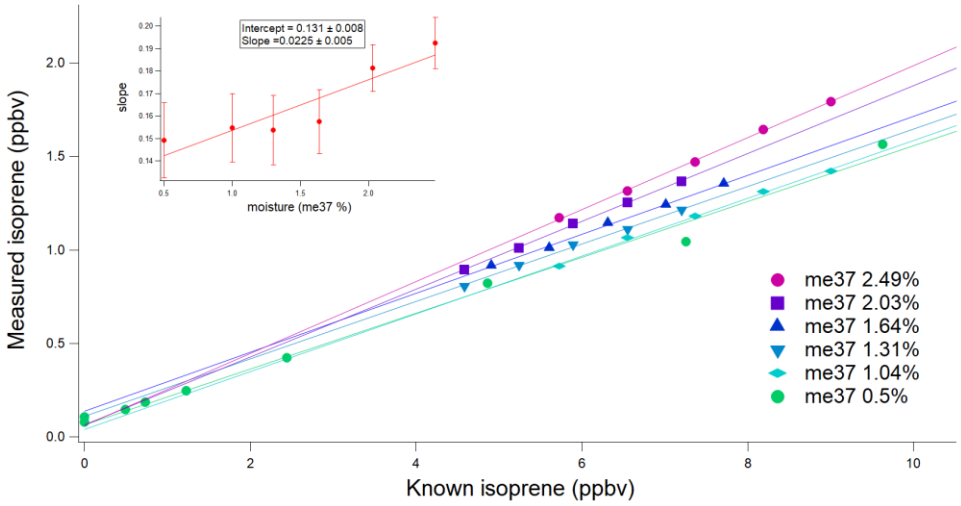

Figure S5: Isoprene gas phase calibrations at different humidities and the dependency of the slope on the measured humidity as an inset. Error bars represent 95% confidence intervals of the linear regression.

For benzene and toluene, the calibration slopes decrease with increasing humidity (Fig. S3 and Fig. S4) because they possess intermediate proton affinities and are ionized by the primary ion but not by the primary ion water cluster (Warneke et al., 2001). The primary ion water cluster is more stable, because the additional water cluster stabilizes the positive charge (Blake et al., 2009).

For isoprene, the opposite effect is observed and the calibration slope increases with increasing humidity (Fig. S5). Here the additional water clusters reduce the fragmentation of isoprene and thus increase the yield of the primary ion at m/z 69. Note that humidity dependant fragmentation of isoprene in PTR-MS has been observed before (Schwarz et al., 2009). Other masses that isoprene fragment ions can be found are m/z 39 and m/z 41.

To further investigate the fragmenting behaviour of isoprene, the same known amount of gas standard was measured at different voltages in the drift tube and ions at mass 41 and 69 were monitored (Fig. S6).

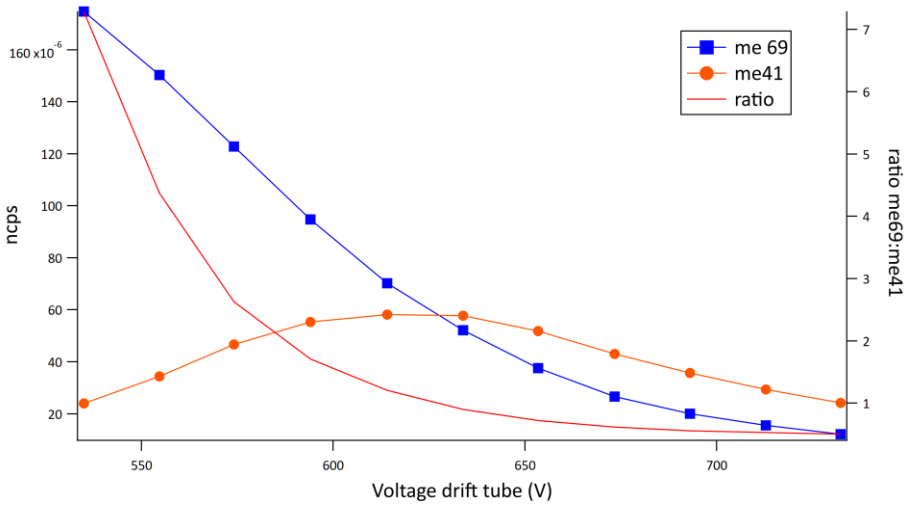

Figure S6: Normalized counts per second of the isoprene primary ion at m/z 69 to the fragment ion at m/z 41 as a function of drift tube voltage. The ratio of the two ions is plotted along.

At higher voltages, the abundance of m/z 69 rapidly decreases, supporting that isoprene is fragmenting in the drift tube. This fragmentation ratio was found to be very stable and vary by less

than 5% over one month for twice weekly calibrations. The remaining isoprene molecules probably reside at m/z 39, which was found to be the dominant ion in this fragmentation (Schwarz et al., 2009). We have accounted for fragmentation in the isoprene measurements presented here.

Supplementary material S3: Map of the cruise track of the selection of data presented here

A map of the cruise track of the underway data presented here is shown in Fig. S7.

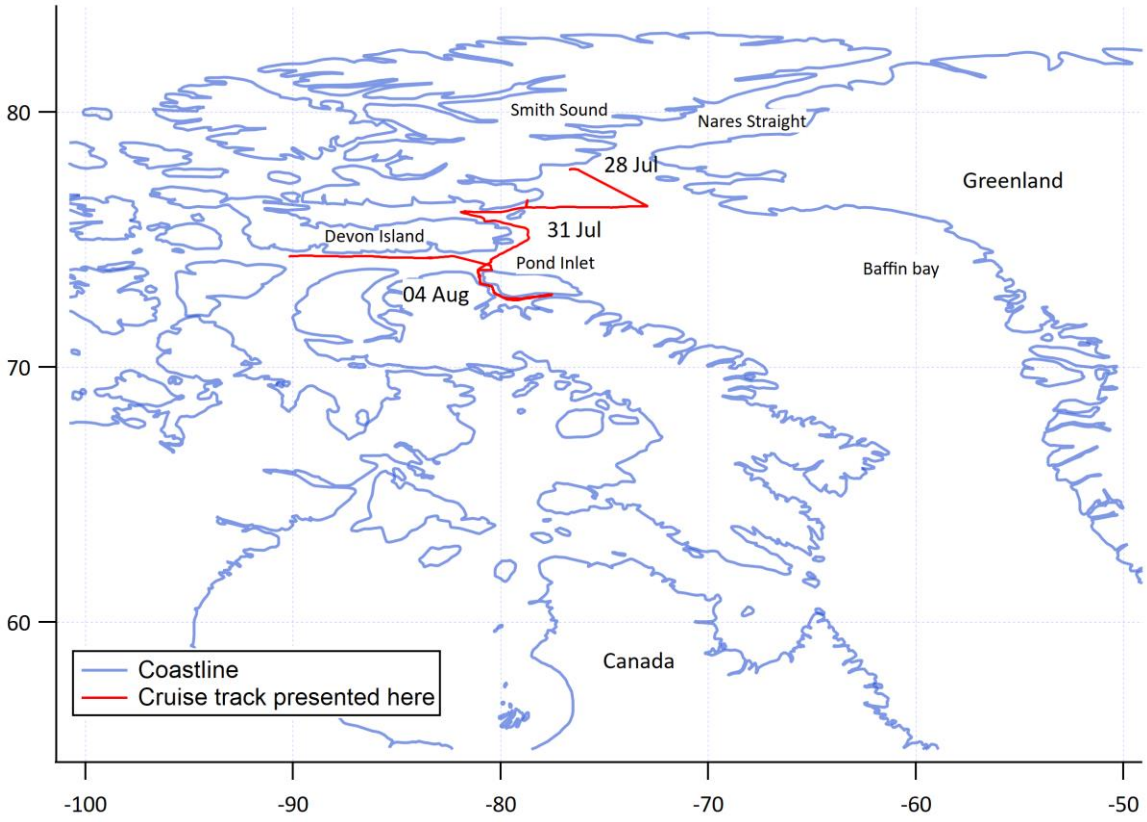

Figure S7: Cruise track of the data presented here.

Supplementary material S4: Derivation of the purging factor

As mentioned in the main paper in Sect. 3.2, the dissolved gas concentrations after equilibration in the coil are computed using equilibrator headspace mixing ratios. However, a solubility-dependent fraction of dissolved VOCs is transferred into the gas phase during the equilibration process. Thus the final dissolved gas concentration will be somewhat lower than the initial concentrations. To account for the removal of a fraction of these gases from the seawater during equilibration a purging factor (PF) based on mass conservation is applied. The PF is the ratio between the dissolved gas concentration before and after complete equilibration in the coil:

$$PF = \frac{C_w(before\ equilibration)}{C_w(after\ equilibration)} \quad (S8)$$

, where;

$$C_W(before\ equilibration) = \frac{X_{tot}}{V_W} \quad (S9)$$

Here X_{tot} is the total number of moles in the system and V_W is the volume of water. In the following demonstration, $X_{a_{fin}}$ and $X_{w_{fin}}$ are gas phase and dissolved number of moles of gas after equilibration and V_a is the volume of carrier gas. Thus $X_{a_{fin}}$ is the number of moles measured as equilibrator headspace mixing ratios. Hence;

$$C_W(after\ equilibration) = H * C_a(after\ equilibration)$$

$$\frac{X_{w_{fin}}}{V_w} = H * \frac{X_{a_{fin}}}{V_a}$$

$$X_{w_{fin}} = H * X_{a_{fin}} * \frac{V_w}{V_a} \qquad (S10)$$

Combining $X_{a_{fin}} = \frac{X_{w_{fin}}}{H*\frac{V_w}{V_a}}$ and $X_{tot} = X_{w_{fin}} + X_{a_{fin}}$ $(S11)$ gives;

$$X_{tot} = X_{w_{fin}} + \frac{X_{w_{fin}}}{H*\frac{V_w}{V_a}}$$

$$X_{tot} = \left(1 + \frac{1}{H * \frac{V_w}{V_a}}\right) * X_{w_{fin}}$$

$$X_{w_{fin}} = \frac{X_{tot}}{1 + \frac{1}{H*\frac{V_w}{V_a}}} \qquad (S12)$$

Thus, $C_W(after\ equilibration) = \frac{X_{w_{fin}}}{V_w}$ $(S13)$

Combining Eq. (S12) and (S13) gives $C_W(after\ equilibration) = \frac{X_{tot}}{1+\frac{1}{H*\frac{V_w}{V_a}}} * \frac{1}{V_w}$ $(S14)$

Combining Eq. (S9) and (S14) with Eq. (S8) gives:

$$PF = \frac{\frac{X_{tot}}{V_w}}{\frac{X_{tot}}{1+\frac{1}{H*\frac{V_w}{V_a}}} * \frac{1}{V_w}}$$

$$PF = \frac{X_{tot}}{V_w} * \frac{1 + \frac{1}{H*\frac{V_w}{V_a}} * V_w}{X_{tot}}$$

$$PF = 1 + \frac{1}{H * \frac{V_w}{V_a}} \qquad (S15)$$

At equal zero air/water flow rates, this is simplified to:

$$PF = \frac{C_w(before\ equilibration)}{C_w(after\ equilibration)} = \frac{1}{H} + 1 \qquad (S16)$$

The expected mixing ratios during invasion experiments is calculated by combining Eq. (S10) and (S11);

$$X_{tot} = X_{a_{fin}} + H * X_{a_{fin}} * \frac{V_w}{V_a}$$

$$X_{tot} = X_{a_{fin}} * (1 + H * \frac{V_w}{V_a})$$

$$X_{a_{fin}} = \frac{X_{tot}}{1 + H * \frac{V_w}{V_a}} \quad (S17)$$

, where the total number of moles is the diluted VOC gas standard mixing ratio.

Supplementary material S5: Compilation of published solubilities for methanol, acetone and acetaldehyde

Here we provide more detail on how the evasion standards of methanol, acetone and acetaldehyde were prepared in MilliQ water. For this, 303 mm^3 of pure methanol (For spectroscopy Uvasol) and 55 mm^3 acetone (HPLC standard) were diluted in a 0.5 dm^3 volumetric flask labelled as "A". In a 1 dm^3 volumetric flask labelled "B", 1 cm^3 acetaldehyde (>=99.5%, A.C.S. Reagent) was dissolved as measured out using a 1 cm^3 volumetric flask. A third flask labelled "C" of 0.5 dm^3 was used to further dilute 330 mm^3 of flask "A" and 330 mm^3 of flask "B". Different amounts of the flask labelled "C" were dissolved in 800 cm^3 MilliQ water syphoned into sampling bottles. Standards were typically analysed within 4 h of dissolving the pure OVOC in water. The same 10 dm^3 batch of MilliQ water was used to dissolve the pure standards and it was also syphoned into the sampling bottles. The same MilliQ blank has been subtracted from the measurements of the evasion calibration curves. The same three air displacement micropipettes (20-200 mm^3, 100-1000 mm^3, 0.5-5 cm^3) with plastic tips were used for this dilution. All volumetric flasks were Pyrex class A volumetric glassware backed over night at 80°C. The SFCE was typically purged with MilliQ water for at least 30 min before starting measurement. The solubilities of the OVOCs at 20 °C in MilliQ water used to compute the expected mixing ratio in Fig. 4 are presented in table S18.

Table S18: Table listing experimentally determined air over water dimensionless Henry solubilities of methanol, acetone and acetaldehyde at 20°C in MilliQ water as listed in R. Sander (2015) along with the in-text reference and the computed slope of the response in the SFCE in ppbv $nmol^{-1}$ dm^3. For full reference of the cited solubilities, please refer to R. Sander (2015). Experimentally determined calibration slope for methanol, acetone and acetaldehyde were 0.00786 ±0.00115 ppbv $nmol^{-1}$ dm^3, 0.0469 ±0.0145 ppbv $nmol^{-1}$ dm^3 and 0.0743 ±0.0190 ppbv $nmol^{-1}$ dm^3.

Reference	Henry solubility	Predicted slope ppbv $nmol^{-1}$ dm^3
Methanol		
1. Li et al., (1993)	7378	0.00326
2. Snider and Dawson (1985)	7220	0.00333
3. Rytting et al., (1978)	7378	0.00326
4. Brunett et al., (1963)	7714	0.00312
5. Glew and Moelwyn-Hughes (1953)	7430	0.00324
6. Butler et al., (1935)	7714	0.00312
7. Vitenberg and Dobryakov (2008)	7044	0.00341
8. St.Pierre et al., (2014)	2212	0.01090
9. Helburn et al., (2008)	2616	0.00919
10. Teja et al., (2001)	6716	0.00358
11. Zhou et al., (2000)	8882	0.00271
12. Gupta et al., (2000)	6678	0.00360
13. Altschuh et al., (1999)	5367	0.00448
14. S. P. Sander et al., (2011)	6715	0.00358
Acetone		
15. Benkelberg et al., (1995)	891	0.0269
16. Hoff et al., (1993)	878	0.0274
17. Zhou and Mopper (1990)	1060	0.0227
18. Guitart et al., (1989)	746	0.0322
19. Hellmann et al., (1987)	341	0.0703
20. Snider and Dawson (1985)	802	0.0299

21. Schoene and Steinhanses (1985)	1062	0.0226
22. Sato and Nakajima (1979)	933	0.0258
23. Vittenberg et al., (1975)	813	0.0295
24. Poulain et al., (2010)	946	0.0254
25. Ji and Evans (2007)	863	0.0278
26. Falabella et al., (2006)	744	0.0323
27. Strekowski and George (2005)	914	0.0263
28. Straver and de Loos (2005)	781	0.0308
29. Chai et al., (2005)	748	0.0321
30. Ayuttaya et al., (2001) (EPICS method)	325	0.0737
31. Ayuttaya et al., (2001) (static cell, linear form)	3.0587	5.93
32. Ayuttaya et al., (2001) (direct phase concentration method)	1725	0.0139
33. S. P. Sander et al., (2015)	901	0.0267
Acetaldehyde		
34. Ji and Evans (2007)	527	0.0455
35. Straver and de Loos (2005)	374	0.0641
36. Marin et al., (1999)	510	0.0470
37. Benkelberg et al., (1995)	439	0.0547
38. Zhou and Mopper (1990)	552	0.0435
39. Guitart et al., (1989)	242	0.0991
40. Betterton and Hoffmann (1988)	419	0.0572
41. Snider and Dawson (1985)	408	0.0589
42. Vitenberg et al., (1974)	298	0.0991
40. Betterton and Hoffmann (1988)	419	0.0572
41. Snider and Dawson (1985)	408	0.0589
42. Vitenberg et al., (1974)	298	0.0804
43. Buttery et al., (1969)	487	0.0493
44. S. P. Sander et al., (2011)	444	0.0541

Supplementary material S6: Photographs of the instrument setup

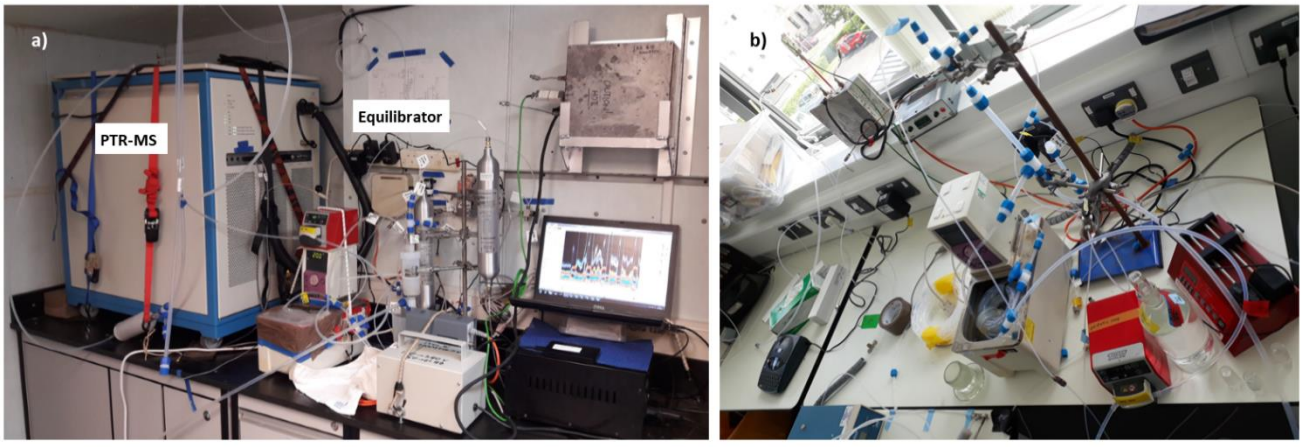

Figure S19: a) Photograph of the instrument setup during deployment on the CCGS *Amundsen* with the jar trap. b) Photograph of the equilibrator in the laboratory post-deployment with the PTFE tee fitting mounted to separate air and water at the end of the segmented flow tube.

Bibliography

Beale, R., Dixon, J. L., Arnold, S. R., Liss, P. S., & Nightingale, P. D.: Methanol, acetaldehyde, and acetone in the surface waters of the Atlantic Ocean, J. Geophys. Res. Ocean., 118, 5412–5425, https://doi.org/10.1002/jgrc.20322, 2013.

Blake, R. S., Monks, P. S., & Ellis, A. M.: Proton-transfer reaction mass spectrometry., Chem. Rev., 109, 861–896, https://doi.org/10.1021/cr800364q, 2009.

Blomquist, B. W., Huebert, B. J., Fairall, C. W., & Faloona, I. C.: Determining the sea-air flux of dimethylsulfide by eddy correlation using mass spectrometry, Atmos. Meas. Tech, 3, 1–20, https://doi.org/10.5194/amtd-2-1973-2009, 2010.

de Gouw, J. a., & Warneke, C.: Measurements of Volatile Organic Compounds In the Earth's Atmosphere using Proton-Trasfer-Reaction Mass Spectrometry, Mass Spectrom. Rev., 26, 223–257, https://doi.org/10.1002/mas, 2007.

Ellis, A. M., & Mayhew, C. A.: *Proton Transfer Reaction Mass Spectrometry: Principles and ApplicationsWiley*, https://doi.org/10.1021/cr800364q, 2014.

Kameyama, S., Tanimoto, H., Inomata, S., Tsunogai, U., Ooki, A., Takeda, S., … Uematsu, M.: High-resolution measurement of multiple volatile organic compounds dissolved in seawater using equilibrator inlet-proton transfer reaction-mass spectrometry (EI-PTR-MS), Mar. Chem., 122, 59–73, https://doi.org/10.1016/j.marchem.2010.08.003, 2010.

Lindinger, W., & Jordan, a.: Proton-transfer-reaction mass spectrometry (PTR–MS): on-line monitoring of volatile organic compounds at pptv levels, Chem. Soc. Rev., 27, 347, https://doi.org/10.1039/a827347z, 1998.

Schwarz, K., Filipiak, W., & Amann, A.: Determining concentration patterns of volatile compounds in exhaled breath by PTR-MS, J. Breath Res., 3, 1–15, https://doi.org/10.1088/1752-7155/3/2/027002, 2009.

Warneke, C., Van Der Veen, C., Luxembourg, S., De Gouw, J. A., & Kok, A.: Measurements of benzene and toluene in ambient air using proton-transfer-reaction mass spectrometry: Calibration, humidity dependence, and field intercomparison, Int. J. Mass Spectrom., 207, 167–182, https://doi.org/10.1016/S1387-3806(01)00366-9, 2001.

Warneke, Carsten, De Gouw, J. A., Kuster, W. C., Goldan, P. D., & Fall, R.: Validation of atmospheric VOC measurements by proton-transfer-reaction mass spectrometry using a gas-chromatographic preseparation method, Environ. Sci. Technol., 37, 2494–2501, https://doi.org/10.1021/es026266i, 2003.

Williams, J., Pöschl, U., Crutzen, P. J., Hansel, A., Holzinger, R., Warneke, C., … Lelieveld, J.: An atmospheric chemistry interpretation of mass scans obtained from a proton transfer mass spectrometer flown over the tropical rainforest of Surinam, J. Atmos. Chem., 38, 133–166, https://doi.org/10.1023/A:1006322701523, 2001.

Yang, M., Beale, R., Smyth, T., & Blomquist, B. W.: Measurements of OVOC fluxes by eddy covariance using a proton-transfer- reaction mass spectrometer-method development at a coastal site, Atmos. Chem. Phys., 13, 6165–6184, https://doi.org/10.5194/acp-13-6165-2013, 2013.

Yang, M., & Fleming, Z. L.: Estimation of atmospheric total organic carbon (TOC) - paving the path towards carbon budget closure, Atmos. Chem. Phys., 19, 459–471, https://doi.org/10.5194/acp-19-459-2019, 2019.

Zhao, J., & Zhang, R.: Proton transfer reaction rate constants between hydronium ion (H3O+) and volatile organic compounds, Atmos. Environ., 38, 2177–2185, https://doi.org/doi: 10.1016/j.atmosenv.2004.01.019, 2004.